Andreev scattering, Josephson currents, and coupling energy in clean superconductor-semiconductor-superconductor junctions

U. Schüssler and R. Kümmel
Physikalisches Institut der Universität Würzburg, D-8700 Würzburg, Germany
(Received 24 August 1992)

Superconductor-semiconductor-superconductor junctions with superconducting Nb banks coupled by the degenerate III-V semiconductor n-type InAs are described by the Bogoliubov-de Gennes equations (BdGE) with spatially and energy-dependent effective masses, abruptly changing conduction-band edges, interface barriers, and vanishing pair potential in the semiconducting (Sm) layer. Phase coherence between the superconducting (S) banks is mediated by Andreev scattering of ballistic quasiparticles, which is the only mechanism considered for Cooper pair transfer. The bound-state subbands, broadened by scattering from the mismatches at the S-Sm interfaces, split off at finite phase differences Φ between the pair potentials in either S region. At arbitrary temperatures T below the critical temperature T_c of Nb, the Josephson-current density $j(\Phi)$, computed numerically from the solutions of the BdGE, can be simulated very well by $j(\Phi)=j_c\sin[\Phi-L_{\rm kin}j(\Phi)]$, where the kinetic-inductance parameter $L_{\rm kin}$ decreases with increasing temperature and decreasing Sm layer thickness $2a$. The maximum coupling energy per unit area is $E_J(\Phi=\pi)=j_c\hbar/e$ for all $L_{\rm kin}$. The critical Josephson-current density j_c is 5.6×10^5 A cm^{-2} at $T=0$ K, $n=10^{19}$ cm^{-3}, $2a=0.3$ μm, and vanishing interface barrier strength Z. j_c decreases with increasing $2a$, T, and Z; the decrease with temperature becomes more and more pronounced as the electron concentration n in the Sm layer decreases; the decrease with Z can be understood by the Z dependence of the Andreev scattering probability. The Josephson currents computed from Andreev scattering are so large that they should destroy any pair potential possibly induced in the Sm layer by the proximity effect.

I. INTRODUCTION

Josephson currents in superconductor-semiconductor-superconductor (S-Sm-S) junctions have been of considerable experimental[1–13] and theoretical[14–21] interest for a long time, not only because S-Sm-S junctions are weak links with interesting properties intermediate between that of tunnel and superconductor–normal-metal–superconductor (S-N-S) junctions, but also because they constitute promising devices for superconducting transistors (Josephson field-effect transistors) of considerable technological potential. While most discussions of the Josephson current in conjunction with experiments have focused on the proximity effect,[1,2,4,6,9–11,22] theories usually neglect the pair potential in the Sm layer.[16–18,21] Only recently, people have begun to look more closely into the question of how the transmission of Cooper pairs and phase coherence across the Sm layer by electron-hole (Andreev) scattering from the spatial variations of the superconducting pair potential[23] determines the electrodynamic properties of S-Sm-S junctions.[12,13,17,19,21,24–27] The purpose of the present paper is a quantitative computation of the Josephson currents and the phase coupling energy in junctions where the degenerate semiconductor n-type InAs is sandwiched between two superconducting Nb contacts, taking into account the isotropic, nonparabolic conduction-band structure of InAs, interface barriers, and the mismatches of the Fermi energies in the S and Sm regions. By choosing a zero pair potential in the Sm layer, we make sure that the only mechanism producing the Josephson effect is Andreev scattering.

II. MODEL

We consider two Nb superconductors (Fermi energy $\varepsilon_{F,S}=5.32$ eV; $T_c=9.2$ K) coupled by the conduction electrons of the degenerate narrow-gap semiconductor n-type InAs, whose electron concentration may vary between $n=10^{16}$ cm^{-3} ($\varepsilon_{F,Sm}=0.007$ eV) and 10^{19} cm^{-3} ($\varepsilon_{F,Sm}=0.411$ eV).

The normal-state bulk properties of the junction materials are given by the following model: The dependence of the energy ξ_{Sm} on the wave vector $\mathbf{k}$ in the isotropic nonparabolic conduction band of InAs is described by a k-dependent effective-mass parameter $\tilde{m}(k^2)$ in the dispersion relation

$$\xi_{Sm}(\mathbf{k})=\xi^0_{Sm}+\frac{\hbar^2k^2}{2\tilde{m}(k^2)}\ , \tag{1}$$

where $\tilde{m}(0)=0.023m_0$ at the Γ point. In niobium we have free electrons of mass m_0 and the dispersion relation $\xi_S(\mathbf{k})=\xi^0_S+\hbar^2k^2/2m_0$. The Fermi energy in the semiconductor $\varepsilon_{F,Sm}$ is defined with the help of Eq. (1) by

$$\varepsilon_{F,Sm}\equiv\xi_{Sm}(k_{F,Sm})-\xi^0_{Sm}=\frac{\hbar^2k^2_{F,Sm}}{2\tilde{m}(k^2_{F,Sm})}\ , \tag{2}$$

with the usual dependence of the Fermi wave number $k_{F,Sm}$ on the electron concentration n for isotropic sys-

tems, $k_{F,Sm}=(3\pi^2 n)^{1/3}$. We have calculated the effective-mass parameter $\tilde{m}(k^2)$ using the Kane-model $\mathbf{k}\cdot\mathbf{p}$ approximation.[28] In Fig. 1 it is shown as the function $m_{Sm}(\varepsilon)$ of $\varepsilon(k)\equiv\hbar^2k^2/2\tilde{m}(k^2)$.

We assume that the S-Sm-S contact is translationally invariant in the x and y directions. In the semiconductor region $-a<z<+a$, the band structure of Eq. (1) is assumed to be valid. All effects of band bending, interface potentials, and lattice mismatches[29] are modeled by the barrier potential[30]

$$U_B(z)=\frac{\hbar^2k_{F,S}}{m_0}Z[\delta(z-a)+\delta(z+a)] , \tag{3}$$

with the Dirac delta function $\delta(z)$; here, Z is a variable barrier-strength parameter and $k_{F,S}=(2m_0\varepsilon_{F,S})^{1/2}/\hbar$. The conduction-band edges ξ_S^0, ξ_{Sm}^0 define a scalar potential which changes discontinuously at the interfaces

$$U_c(z)=\xi_S^0[1-\Theta(a-|z|)]+\xi_{Sm}^0\Theta(a-|z|) , \tag{4}$$

where $\Theta(x)$ is 1 for $x\geq 0$ and zero otherwise.

Since we are only interested in Josephson currents due to Andreev reflections and since the BCS coupling constant and density of states in InAs are small anyway, we disregard the possibility of a pair potential in the Sm layer. Furthermore, because of the large mismatch in the material parameters of metal and semiconductor, the proximity effect in the superconducting banks can be disregarded, too.[16,31] Therefore the model of the superconducting pair potential is

$$\Delta(\mathbf{r},T)=|\Delta(T)|e^{i2\varphi(\mathbf{r})}\Theta(|z|-a) . \tag{5}$$

All magnetic fields are neglected, and the phase difference across the Sm layer is $\Phi=2\varphi(z=+a)-2\varphi(z=-a)$.

In the many-body Hamiltonians $\hat{H}_{Sm}$ and $\hat{H}_S$ of the Sm and S layers, the single-particle operators "kinetic energy plus lattice potential" are replaced by $\xi_{Sm}(-i\nabla)$ and $\xi_S(-i\nabla)$ according to the Wannier theorem,[32] where ξ_{Sm} and ξ_S are given in and below Eq. (1). From these Hamiltonians, Bogoliubov–de Gennes equations (BdGE) (Ref. 33) are derived for quasiparticle (QP) wave functions

$$\Psi(\mathbf{r})=\begin{bmatrix}u(\mathbf{r})\\ v(\mathbf{r})\end{bmatrix} , \tag{6}$$

with energies E. In the homogeneous semiconductor, the QP electron and hole wave functions $u(\mathbf{r})$ and $v(\mathbf{r})$ are plane waves; operating on them, the effective-mass operator $1/\tilde{m}(-\nabla^2)$ turns into the inverse energy-dependent effective masses $1/m_{Sm}(\varepsilon_{F,Sm}+E)$ for electrons and $1/m_{Sm}(\varepsilon_{F,Sm}-E)$ for holes which can be obtained from Fig. 1 with $\varepsilon=\varepsilon_{F,Sm}\pm E$.

In the S-Sm-S junction, the QP wave functions are described by the BdGE

$$\begin{bmatrix}H_0^+ +H_I^+ & |\Delta|\\ |\Delta| & -H_0^- +H_I^-\end{bmatrix}\Psi=E\Psi , \tag{7}$$

where $H_0^{\pm}$ has a form which corresponds to the model effective-mass Hamiltonians for abrupt heterojunctions of Morrow and Brownstein:[34]

$$H_0^{\pm}=-\frac{\hbar^2}{2}\nabla\frac{1}{m^{\pm}(z)}\nabla+U_c(z)+U_B(z)-\mu ; \tag{8}$$

μ is the chemical potential. The z-dependent effective masses are defined as

$$m^{\pm}(z)\equiv m_0[1-\Theta(a-|z|]+m_{Sm}(\varepsilon_{F,Sm}\pm E)\Theta(a-|z|) . \tag{9}$$

We use a gauge where the pair potential is real, so that the current in the junction gives rise to

$$H_I^{\pm}=\frac{1}{2}\left[\mathbf{v}_\varphi^{\pm}\frac{\hbar}{i}\nabla+\frac{\hbar}{i}\nabla\mathbf{v}_\varphi^{\pm}\pm m^{\pm}(\mathbf{v}_\varphi^{\pm})^2\right] , \tag{10}$$

with the "superfluid" velocity

$$\mathbf{v}_\varphi^{\pm}\equiv\frac{\hbar}{m^{\pm}}\left\{\nabla\varphi[1-\Theta(a-|z|)]+\mathbf{e}_z\frac{\Phi}{4a}\Theta(a-|z|)\right\} . \tag{11}$$

By integrating the BdGE, we obtain as matching conditions at the S-Sm interfaces in $z=\pm a$ that Ψ has to be continuous and that

$$\hat{W}\Psi|_{z=\pm a+0}-\hat{W}\Psi|_{z=\pm a-0}=\frac{2k_{F,S}}{m_0}Z\Psi|_{z=\pm a} , \tag{12}$$

with

$$\hat{W}\equiv\left[\frac{i}{\hbar}\mathbf{e}_z\begin{bmatrix}\mathbf{v}_\varphi^+ & 0\\ 0 & -\mathbf{v}_\varphi^-\end{bmatrix}+\begin{bmatrix}1/m^+ & 0\\ 0 & 1/m^-\end{bmatrix}\frac{\partial}{\partial z}\right] . \tag{13}$$

The current density $\mathbf{j}_{Sm}$ in the Sm layer is obtained from the continuity equation $i\langle[\hat{\rho},\hat{H}_{Sm}]\rangle_{S\text{-}Sm\text{-}S}=-\hbar\,\mathrm{div}\,\mathbf{j}_{Sm}$, where $\hat{H}_{Sm}$ is the effective-mass Hamiltonian in the Sm layer, $\hat{\rho}$ is the charge-density operator, and the average is computed with the states of the S-Sm-S junction. This re-

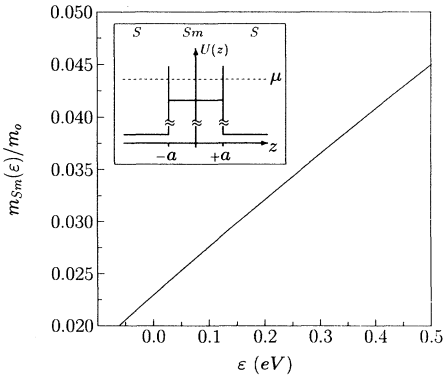

FIG. 1. Energy-dependent effective-mass parameter $m_{Sm}(\varepsilon)$ in the nonparabolic conduction band of n-type InAs. The electron energy ε is measured relative to the conduction-band minimum ξ_{Sm}^0 at the Γ_6 point of the Brillouin zone; the range $\varepsilon<0$ corresponds to evanescent states in the Sm layer (Ref. 28). The inset shows the spatial variation of the scalar potential $U(z)=U_c(z)+U_B(z)$ representing conduction-band edges and interface barriers in the S-Sm-S junction; μ is the chemical potential.

sults in

$$\mathbf{j}_{\mathrm{Sm}}=-e2\,\mathrm{Re}\left\{\sum_n\left[f(E_n)u_n^*\left[\frac{\hbar}{im^+}\nabla+\mathbf{v}_\varphi^+\right]u_n\right.\right.$$
$$+[1-f(E_n)]$$
$$\left.\left.\times v_n\left[\frac{\hbar}{im^-}\nabla+\mathbf{v}_\varphi^-\right]v_n^*\right]\right\}, \qquad (14)$$

which is a generalization of the supercurrent density in the jellium model.[35] $f(E)$ is the Fermi distribution function, and u_n and v_n are the QP eigenfunctions of energy E_n.

III. RESULTS

The normalized solutions of Eqs. (7)–(11), $u_n(\mathbf{r})$ and $v_n(\mathbf{r})$, and their energies E_n are computed numerically from the system of linear equations which result from matching the plane-wave solutions in the S and Sm layers at the interfaces. The index n stands for the triple of quantum numbers k_x, k_y, and l, where k_x and k_y are the wave numbers of the propagation parallel to the junction interfaces and l labels the energies of the bound and scattering states at constant k_x and k_y. In the S regions, $\mathbf{v}_\varphi^\pm$ can be neglected,[16–18,20] because the electron concentration is at least two orders of magnitude higher than in the Sm layer; furthermore, the width D of the superconductors in x,y direction is assumed to be much larger than the London penetration depth λ, so that the interior of the S regions is current free. The calculations are done for different material parameters, temperatures T, and phase differences Φ.

For QP energies $E<|\Delta(T)|$, bound states with a discrete energy spectrum exist in the Sm layer, similar to the situation in metallic weak links (S-N-S).[36] However, the bound-state energies E, shown in Fig. 2 as functions of $k_{z\mathrm{F}}=(k_{\mathrm{F,Sm}}^2-k_x^2-k_y^2)^{1/2}$, differ significantly from the ones of S-N-S junctions.[37] This is due to the competition between Andreev scattering from the spatial variations of the pair potential and normal scattering from the mismatches of Fermi energies and effective masses at the interfaces [Fig. 2(a)]. The energy dependence of the effective masses must be treated carefully: Slight inconsistencies already change the initial curvatures of the $E(k_{z\mathrm{F}})$ branches[37] from the correct ones shown in Fig. 2. Additional surface barriers ($Z>0$) further suppress Andreev scattering [Fig. 2(b)]. For $Z\gg1$ one gets the usual particle-in-a-box spectrum of an isolated Sm layer of thickness $2a$. Symmetry breaking by current flow at finite phase differences $0<\Phi<\pi$ results in the splitting of the $E(k_{z\mathrm{F}})$ branches shown in Fig. 2(c); here, the degeneracy of the odd- and even-parity states of Figs. 2(a) and 2(b) is removed. At phase differences $\Phi=\pi$ (when the Josephson current vanishes), degeneracy is reestablished, and the lowest $E(k_{z\mathrm{F}})$ branch touches the $E=0$ axis [Fig. 2(d)].

With the numerically computed QP wave functions for the bound and scattering states and their corresponding energies, the current density in the Sm layer is numerically computed from Eq. (14) as a function of the phase

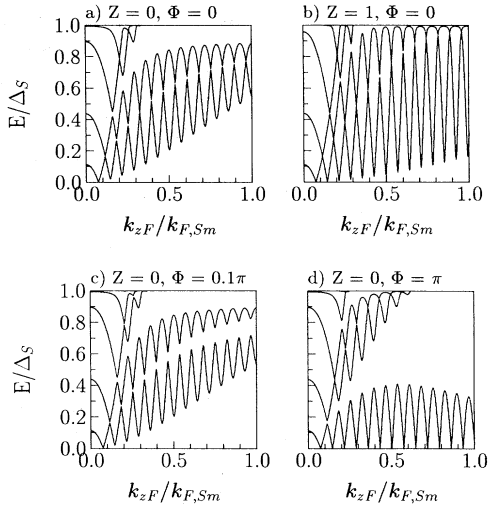

FIG. 2. Discrete energy spectra of the bound states $E(k_{z\mathrm{F}})<\Delta_S\equiv|\Delta(0)|$ of a Nb/n-type InAs/Nb junction of Sm thickness $2a=0.3\ \mu$m and electron concentration $n=10^{17}\ \mathrm{cm}^{-3}$ at $T=0$ K for various interface barrier strengths Z and phase differences Φ.

difference Φ. Typical results for various temperatures are shown in Fig. 3.

With increasing temperature the j-Φ dependence approaches the sinΦ behavior of tunneling junctions. The numerical results can be simulated by a two-parameter analytic expression which is similar to the one suggested by Likharev:[38]

$$j(\Phi)=j_c\sin[\Phi-L_{\mathrm{kin}}j(\Phi)]\ . \qquad (15)$$

The two parameters are the critical-current density j_c and the kinetic-inductance parameter L_{kin}, both depending on the temperature and S-Sm-S material parameters.

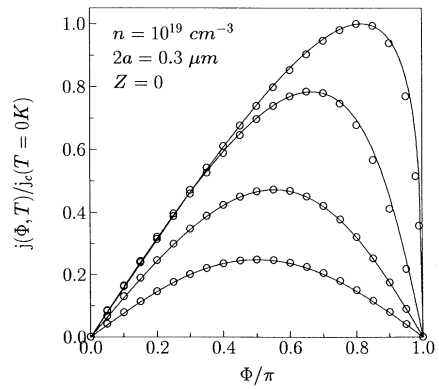

FIG. 3. Current-phase relationship in a Nb/n-type InAs/Nb junction for temperatures $T/T_c=0.0$, 0,2, 0.4, and 0.6 (top to bottom; $T_c=9.2$ K). Circles represent the numerical results, and the solid lines show the fit according to Eq. (15) with $L_{\mathrm{kin}}/(10^{-6}\ \mathrm{cm}^2\mathrm{A}^{-1})=1.8$, 1.2, 0.6, and 0.0. The zero-temperature critical current is $j_c(T=0\ \mathrm{K})=5.6\times10^5\ \mathrm{A\,cm}^{-2}$.

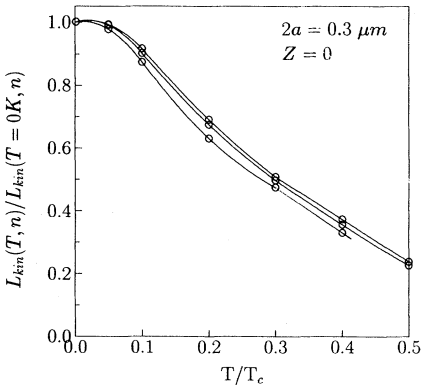

FIG. 4. Temperature dependence of the normalized kinetic-inductance parameter $L_{\rm kin}$ for Sm electron concentrations $n=10^{18}$, 10^{19}, and 10^{17} cm^{-3} (top to bottom) with $L_{\rm kin}(T=0\ {\rm K},n)=1.0\times10^{-5}$, 1.8×10^{-6}, and 7.4×10^{-5} cm^{2}A^{-1}, respectively. Circles represent the numerical results, and the solid lines are interpolations.

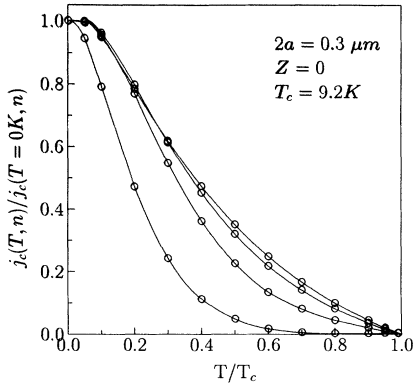

FIG. 6. Temperature dependence of the critical-current density j_c for Sm electron concentrations $n=10^{19}$, 10^{18}, 10^{17}, and 10^{16} cm^{-3} (from top to bottom at $T=0.6T_c$) with $j_c(T=0\ {\rm K},n)=5.6\times10^5$, 8.3×10^4, 6.4×10^3, and 3.3×10^2 A cm^{-2}. The circles represent the numerical results, and the solid lines are interpolations.

The temperature dependence of $L_{\rm kin}$ shown in Fig. 4 is practically the same for all Sm electron concentrations n in the range $10^{17}\le n\le10^{19}$ cm^{-3}. $L_{\rm kin}$ increases with the Sm layer thickness $2a$ and decreases with electron concentration n; qualitatively, this behavior is the same as that of the kinetic inductance of homogeneous superconductors.[39]

With increasing temperature the coupling energy per unit area of the junction,

$$E_J(\Phi)\equiv\frac{\hbar}{2e}\int_0^{\Phi}j(\Phi')d\Phi' , \tag{16}$$

shown in Fig. 5, decreases, and the shape of the $E_J(\Phi)$ curves changes from nearly parabolic to a cosΦ behavior as $L_{\rm kin}j(\Phi)$ decreases with T. This is similar to the change of the energy-crystal momentum relation of a single electron in a periodic potential as one goes from the nearly-free-electron limit to the tight-binding approximation. Note that, even when for $L_{\rm kin}\neq0$ the shape of $E_J(\Phi)$ differs significantly from the cosΦ behavior of Josephson tunnel junctions, the maximum coupling energy $E_J(\pi)$ is independent from $L_{\rm kin}$ and given by $E_J(\pi)=\hbar j_c/e$, as can be derived from Eqs. (15) and (16) by direct integration with appropriate substitutions.

The dependence of the critical-current density j_c on temperature T, electron concentration n, barrier strength Z, and Sm layer thickness $2a$ is shown in Figs. 6–8.

From the rapid decrease with temperature of the critical current at $n=10^{16}$ cm^{-3} in Fig. 6, we note that in S-Sm-S junctions with small n the dissipation free current may approach zero at temperatures considerably lower than the critical temperature T_c of the superconducting material. Therefore a vanishing of the dissipation free current in an S-Sm-S junction does not necessarily imply

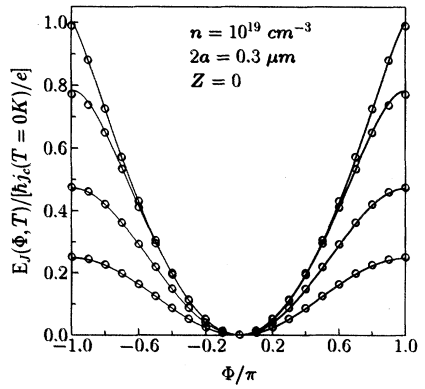

FIG. 5. Coupling energy $E_J(\Phi)$ for the same material and temperature parameters as in Fig. 3 with the same meaning of circles and solid lines. $\hbar j_c(T=0\ {\rm K})/e=2.3\times10^9$ eV cm^{-2}.

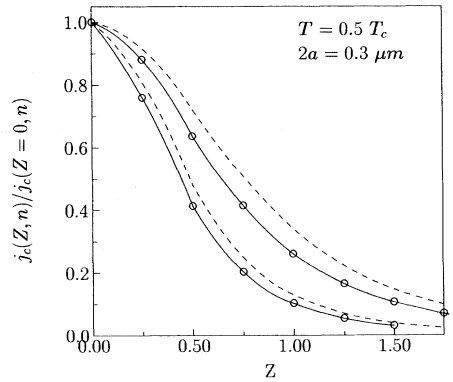

FIG. 7. Critical-current density as a function of the barrier strength Z for $n=10^{19}$ cm^{-3} (top curve) and $n=10^{17}$ cm^{-3} (bottom curve), with $j_c(Z=0,n)=2.0\times10^5$ and 1.5×10^3 A cm^{-2}. The circles represent the numerical results, and the solid lines are interpolations. The dashed lines show the squared normalized transmission probabilities $[T(Z,n)/T(Z=0,n)]^2$ of normal electrons (at $T>T_c$) computed for one S-Sm interface.

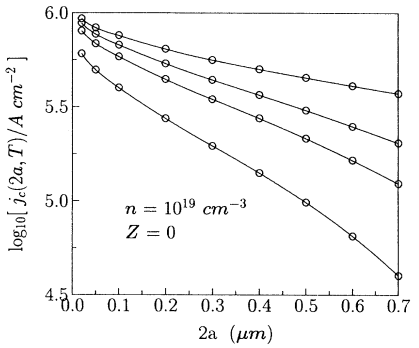

FIG. 8. Critical-current density as a function of the Sm layer thickness $2a$ for $T/T_c=0.0$, 0.2, 0.3, and 0.5 (top to bottom). The circles represent the numerical results, and the solid lines are interpolations.

the vanishing of the superconducting properties of the metal layers.

Figure 7 shows that the critical current decreases with the interface barrier strength Z in the same way as the squared electron transmission probability $T(Z)^2$ does. This behavior can be understood by the $T(Z)^2$ dependence of the Andreev-scattering probability.[26] The transmission probability of an electron at normal incidence on the interface between n-type InAs and Nb in the normal state is

$$T(Z)=\left[\frac{1}{4}\left[\chi+\frac{1}{\chi}\right]^2+\left[\frac{Z}{\chi}\right]^2\right]^{-1}, \tag{17}$$

with

$$\chi=\left[\frac{\hbar k_{\mathrm{F,Sm}}/m_{\mathrm{Sm}}(\varepsilon_{\mathrm{F,Sm}})}{\hbar k_{\mathrm{F,S}}/m_0}\right]^{1/2}, \tag{18}$$

being given by the ratio of the Sm and S Fermi velocities.

The logarithmic plot of the critical current as a function of the Sm layer thickness $2a$ in Fig. 8 shows that the computed decrease of j_c can be approximated by the exponential function $\exp[-2a/l(T)]$ with a temperature-dependent decay length $l(T)$. Such exponential decay has been observed in experiments on Nb/n-type InAs/Nb (Refs. 1–4 and 6) and other S-Sm-S junctions[9,10] and is often discussed in conjunction with the proximity effect. However, quantitative discrepancies in the decay lengths are noted.[10,22] Previous Green's-function theories of S-N-S junctions[16,17] find an exponential decrease of j_c with $2a/\xi_T$, $\xi_T=\hbar v_N/2\pi k_B T$, in the limit $2a \gg \xi_T$. This limit is not satisfied in our S-Sm-S junctions, and l has neither the magnitude nor the temperature dependence of ξ_T.

IV. DISCUSSION AND CONCLUSION

Inoue and Kawakami[5] observed a critical Josephson-current density $j_c=4.7\times10^3$ A cm^{-2} in a sandwichlike Nb/n-type InAs/Nb junction of Sm layer thickness $2a=0.3$ μm and carrier concentration $n=2\times10^{18}$ cm^{-3} at $T=2.1$ K. From their diffusion coefficient and Fermi velocity, we estimate an elastic mean free path $l\approx0.6$ μm$>2a$. From our theory we compute a critical Josephson-current density of $j_c=1.2\times10^5$ A cm^{-2} for the same $2a,n,T$ and for $Z=0$. j_c falls off to the experimentally observed magnitude, if we choose $Z\approx2$. It is reasonable to assume the presence of interface barriers in the experimental S-Sm-S junctions, because the measured critical currents have been found to depend sensitively on the interface preparation[1,4] and vary from sample to sample.[5]

According to the Silsbee criterion or the thin-film pair-breaking criterion,[33,40] the critical-current density in Nb with $\Delta_S\equiv|\Delta(T=0\ \mathrm{K})|=1.5$ meV and electron concentration $n_S=5.56\times10^{22}$ cm^{-3} is

$$j_{c,\mathrm{Nb}}(T=0\ \mathrm{K})\approx2\times10^8\ \mathrm{A/cm^2}\ .$$

Thus the maximum density of uniform current flow in the Sm layer is

$$j_{\mathrm{Sm,max}}\approx j_{c,\mathrm{Nb}}(\lambda/D)>10^6\ \mathrm{A/cm^2}$$

for $D\le10^2\lambda$. The Josephson-current densities calculated by us are below that limit (see Fig. 8). The same pair-breaking criteria can be used in order to estimate what a finite, proximity-induced pair potential Δ_{Sm} in the Sm layer might contribute to the critical Josephson current. Δ_{Sm} will be destroyed by current densities exceeding

$$j_P=j_{c,\mathrm{Nb}}(n/n_S)^{2/3}(\Delta_{\mathrm{Sm}}/\Delta_S)\ .$$

For Sm electron concentrations[1–6] $n\le10^{19}$ cm^{-3}, one has $(n/n_S)^{2/3}\le3\times10^{-3}$. From Kieselmann's[41] self-consistent calculations of the pair potential in proximity contacts at arbitrary temperatures, as well as from the proximity-effect theory for $(1-T/T_c)\ll1$,[5,42,43] we expect that in the Sm layer with $\varepsilon_{\mathrm{F,Sm}}\ll\varepsilon_{\mathrm{F,S}}$ any induced pair potential Δ_{Sm} is considerably smaller than Δ_S. Even with Δ_{Sm} as big as $0.1\Delta_S$, for $n=10^{19}$ cm^{-3}, $2a=0.3$ μm, and $T=0$ K, the pair-breaking current density j_P would be 6×10^4 A cm^{-2} and thus an order of magnitude smaller than the critical Josephson-current density $j_c=5.6\times10^5$ A cm^{-2} calculated by us for the same parameters on the basis of Andreev scattering, neglecting Δ_{Sm}. Therefore we believe that in the interpretation of experimentally observed Josephson currents in S-Sm-S junctions Andreev scattering deserves at least as much attention as the proximity effect.

ACKNOWLEDGMENT

The authors gratefully acknowledge support by the Deutsche Forschungsgemeinschaft and the Rechenzentrum der Universität Würzburg.

[1]T. Kawakami and H. Takayanagi, Appl. Phys. Lett. **46**, 92 (1985).
[2]T. Kawakami and H. Takayanagi, Phys. Rev. Lett. **54**, 2449 (1985).
[3]A. W. Kleinsasser, T. N. Jackson, G. D. Pettit, H. Schmid, J. M. Woodall, and D. P. Kern, Appl. Phys. Lett. **49**, 1741 (1986).
[4]T. Kawakami and H. Takayanagi, Jpn. J. Appl. Phys. **26**, Suppl. 26-3, 2059 (1987).
[5]K. Inoue and T. Kawakami, J. Appl. Phys. **65**, 1631 (1989).
[6]T. Akazaki, T. Kawakami, and J. Nitta, J. Appl. Phys. **66**, 6121 (1989).
[7]Ch. Nguyen, J. Werking, H. Kroemer, and E. L. Hu, Appl. Phys. Lett. **57**, 87 (1990).
[8]A. Serfaty, J. Aponte, and M. Octavio, J. Low Temp. Phys. **63**, 23 (1986).
[9]M. Hatono, T. Nishino, F. Murai, and U. Kawabe, Appl. Phys. Lett. **53**, 409 (1988).
[10]T. Hato, H. Akaike, A. Fujimaki, and H. Hayakawa, IEEE Trans. Magn. **27**, 2585 (1991).
[11]D. R. Heslinga, Ph.D. theses, University of Groningen, 1991.
[12]W. M. van Huffelen, T. M. Klapwijk, and L. de Lange, Phys. Rev. B **45**, 535 (1992).
[13]W. M. van Huffelen, T. M. Klapwijk, D. R. Heslinga, M. J. de Boer, and N. van der Post (unpublished).
[14]J. Seto and T. van Duzer, in *Low Temperature Physics—LT 13,* edited by K. D. Timmerhaus, W. J. O'Sullivan, and E. F. Hammel (Plenum, New York, 1974), Vol. 3, pp. 328–333.
[15]P. Seidel and J. Richter, Wiss. Z. Friedrich-Schiller-Univ. Jena, Math.-Naturwiss. Reihe **27**, 291 (1978).
[16]M. Yu. Kupriyanov, Fiz. Nizk. Temp. **7**, 700 (1981) [Sov. J. Low Temp. Phys. **7**, 342 (1981)].
[17]A. Furusaki and M. Tsukada, Physica B **165&166**, 967 (1990); Phys. Rev. B **43**, 10 164 (1991); Solid State Commun. **78**, 299 (1991).
[18]L. G. Aslamazov and M. V. Fistul, Zh. Eksp. Teor. Fiz. **81**, 382 (1981) [Sov. Phys. JETP **54**, 206 (1981)].
[19]V. Z. Kresin, Phys. Rev. B **34**, 7587 (1986).
[20]M. Yu. Kupriyanov and V. F. Lukichev, Zh. Eksp. Teor. Fiz. **94**, 139 (1988) [Sov. Phys. JETP **67**, 1163 (1988)].
[21]B. J. van Wees, K.-M. H. Lenssen, and C. J. P. M. Harmans, Phys. Rev. B **44**, 470 (1991).
[22]A. W. Kleinsasser, J. Appl. Phys. **69**, 4146 (1991).
[23]A. F. Andreev, Zh. Eksp. Teor. Fiz. **46**, 1823 (1964) [Sov. Phys. JETP **19**, 1228 (1964)]; **49**, 655 (1965) [**22**, 455 (1966)].
[24]A. W. Kleinsasser, T. N. Jackson, D. McInturff, F. Rammo, G. D. Pettit, and J. M. Woodall, Appl. Phys. Lett. **55**, 1909 (1989).
[25]T. Nishino, M. Hatano, H. Hasegawa, T. Kure, and F. Murai, Phys. Rev. B **41**, 7274 (1990).
[26]A. W. Kleinsasser, T. N. Jackson, D. McInturff, F. Rammo, G. D. Pettit, and J. M. Woodall, Appl. Phys. Lett. **57**, 1811 (1990).
[27]J. Nitta, H. Nakano, T. Akazaki, and H. Takayanagi, in SQUID '91 (in press).
[28]G. Bastard, *Wave Mechanics Applied to Semiconductor Heterostructures* (Les Editiones de Physique, Les Ulis, France, 1988).
[29]T. Akazaki, J. Nitta, and H. Takayanagi, Appl. Phys. Lett. **59**, 2037 (1991).
[30]G. E. Blonder, M. Tinkham, and T. M. Klapwijk, Phys. Rev. B **25**, 4515 (1982).
[31]W. M. van Huffelen, T. M. Klapwijk, and E. P. Th. M. Suurmeijer (unpublished).
[32]J. M. Ziman, *Electrons and Phonons* (Oxford University Press, Oxford, 1963).
[33]P. G. deGennes, *Superconductivity of Metals and Alloys* (Benjamin, New York, 1966).
[34]R. A. Morrow and K. R. Brownstein, Phys. Rev. B **30**, 678 (1984).
[35]R. Kümmel, Z. Phys. **218**, 472 (1969).
[36]J. Bardeen and J. L. Johnson, Phys. Rev. B **5**, 72 (1972).
[37]R. Kümmel, U. Schüssler, U. Gunsenheimer, and H. Plehn, Physica C **185-189**, 221 (1991).
[38]K. K. Likharev, Rev. Mod. Phys. **51**, 101 (1979).
[39]R. Meservey and P. M. Tedrow, J. Appl. Phys. **40**, 2028 (1969).
[40]J. Bardeen and M. J. Stephen, Phys. Rev. **140**, A1197 (1965).
[41]G. Kieselmann, Phys. Rev. B **35**, 6762 (1987).
[42]G. Deutscher and P. G. deGennes, in *Superconductivity,* edited by R. D. Parks (Dekker, New York, 1969), Vol. 2, pp. 1005–1034.
[43]Y. Tanaka and M. Tsukada, Phys. Rev. B **37**, 5087 (1988); **37**, 5095 (1988).